Supporting Information

Enhancement mechanism of sulfur dopant on catalytic activity of N and P co-doped three-dimensional hierarchically porous carbon as metal-free oxygen reduction electrocatalyst

Yongxi Zan [a,b], Zhengping Zhang [a,b], Meiling Dou [a,b,] and Feng Wang [a,b,*]*

[a] State Key Laboratory of Chemical Resource Engineering, Laboratory of Electrochemical Process and Technology for materials, Beijing University of Chemical Technology, Beijing 100029, China

[b] Beijing Advanced Innovation Center for Soft Matter Science and Engineering, Beijing University of Chemical Technology, Beijing 100029, China

Corresponding author: Prof. Feng Wang. Tel.&Fax.: +86-10-64451996. E-mail: wangf@mail.buct.edu.cn; Dr. Meiling Dou, douml@mail.buct.edu.cn;

Table of Contents

1. General methods

Materials

The dried cattle bone powder was purchased from market in Beijing. Phytic acid (PA), dicyandiamide (DCDA), thiourea (THU), methanol, ethanol, and KOH were purchased from Sinopharm. Nafion (5 wt. %) and high-purity Ar gas were brought from DuPont and Beijing AP BAIF Gases Industry Co., Ltd, respectively. All chemicals were of analytical grade and applied without further purification. Ultrapure water (Millipore, 18.2 MΩ cm) was used for the material preparation.

Electrochemical measurement

RDE measurement: The transferred electron number for the ORR was estimated by the Koutecky-Levich (K-L) equation [S1]:

$$j^{-1} = j_k^{-1} + 1 \Big/ \left(0.2nFC_{O_2}D_{O_2}{}^{2/3}\upsilon^{-1/6}\omega^{1/2}\right) \tag{1}$$

where, j_k is the kinetic current density, j is the measured current density normalized to the geometry surface area of the electrode, n is transferred electron number for the ORR process per oxygen molecule, F is the Faraday constant (96485 C mol^{-1}), D_{O_2} is the diffusion coefficient, υ is the kinematic viscosity, C_{O_2} represents the bulk concentration of O_2, and ω is the rotation rate. The following values are referred when calculating the transferred electron number: $D_{O_2} = 1.9\times 10^{-5}$ cm^2 s^{-1}, $\upsilon = 0.01$ cm^2 s^{-1}, $C_{O_2} = 1.2 \times 10^{-6}$ mol cm^{-3}. The constant of 0.2 is adopted as the rotation rate is expressed in rpm. According to the K-L equation, n can be calculated from the slope of j^{-1} plotted against $\omega^{-1/2}$. For the Tafel plot, the j_k was calculated based on the following equation:

$$j_k = \frac{j \times j_d}{j_d - j} \tag{2}$$

where, j_d is the diffusion limiting current density.

RRDE measurement: For the RRDE measurement, the disk electrode was scanned at a rate of 5 mV s^{-1} and the ring potential was set constant at 1.5 V. The $\% HO_2^-$ and n were determined by the followed equations:

$$\% HO_2^- = 200 \frac{I_r/N}{I_d + I_r/N} \tag{3}$$

$$n = 4 \frac{I_d}{I_d + I_r/N} \tag{4}$$

where, I_d is disk current, I_r is ring current, and N is current collection efficiency of the Pt ring (N=0.40).

2. Supplementary Figures

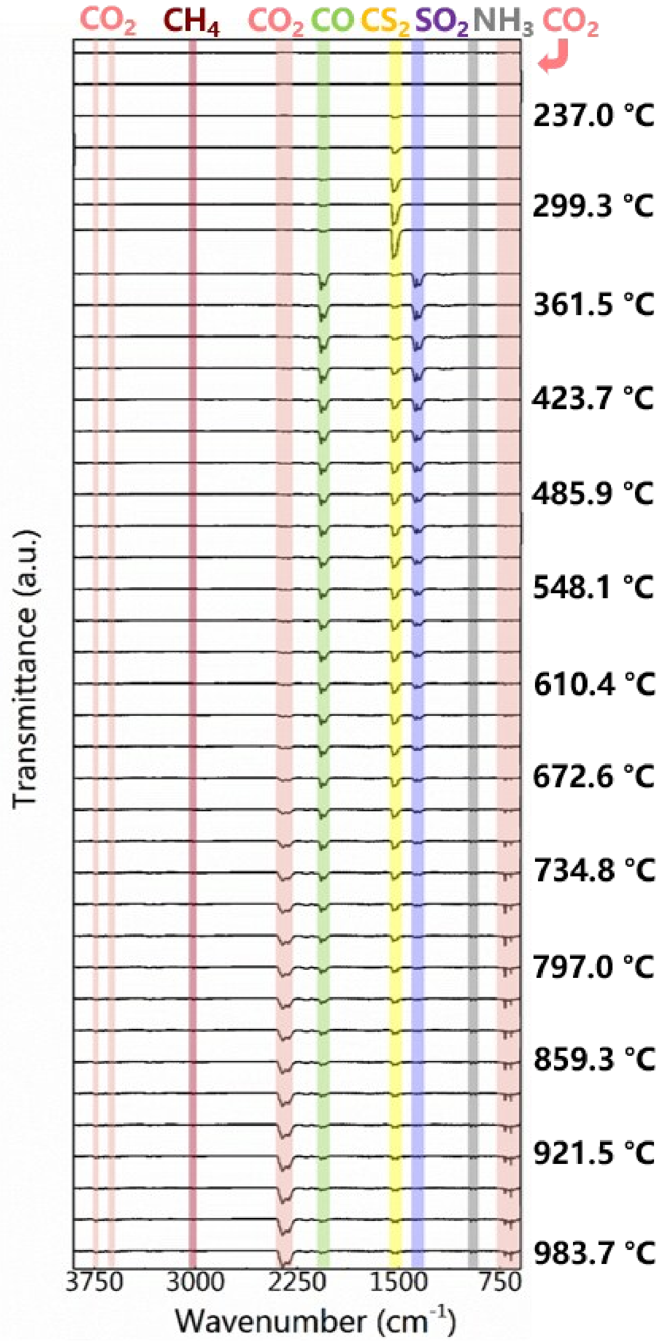

Figure S1. FT-IR spectra at different temperature during the co-pyrolysis process of N,P-HPC and THU for the preparation of S,N,P-HPC-1.

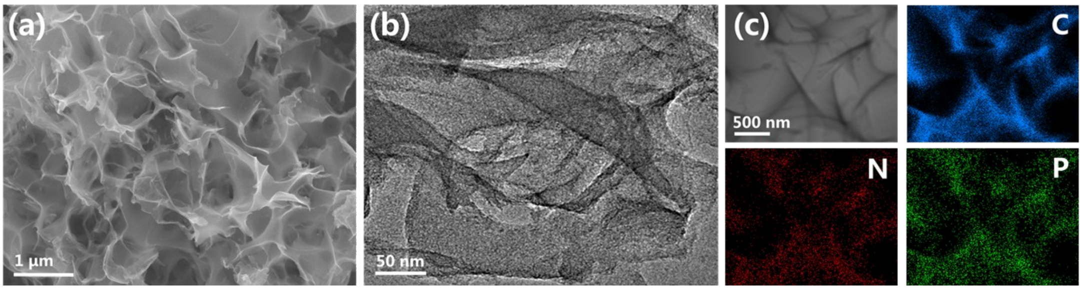

Figure S2. Representative SEM and TEM images of (a, b) N,P-HPC. (c) TEM and corresponding element mapping images of N,P-HPC.

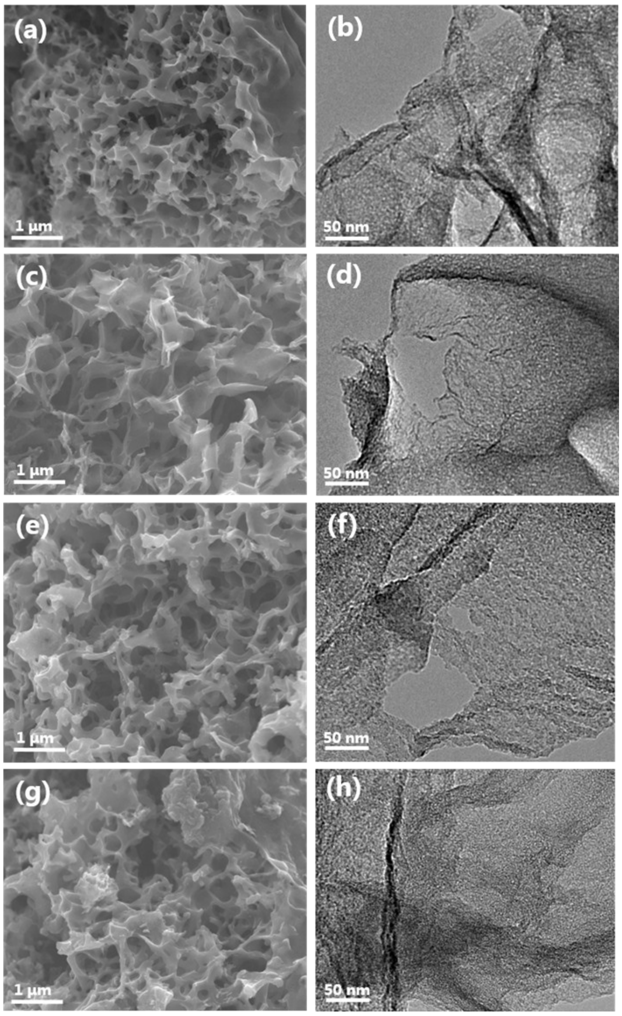

Figure S3. Representative SEM and TEM images of (a, b) S,N,P-HPC-0.5, (c, d) S,N,P-HPC-1, (e, f) S,N,P-HPC-1.5, and (g, h) S,N,P-HPC-2.

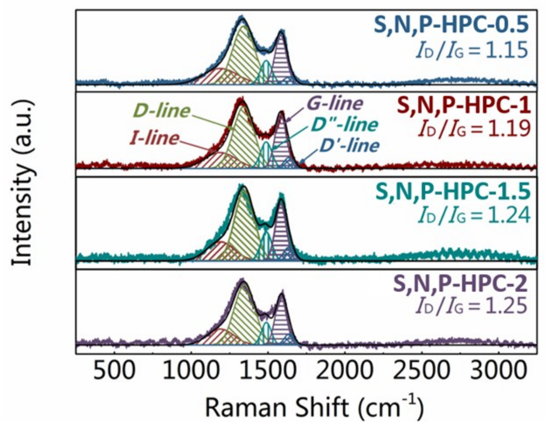

Figure S4. Raman spectras of S,N,P-HPC-0.5, S,N,P-HPC-1, S,N,P-HPC-1.5 and S,N,P-HPC-2.

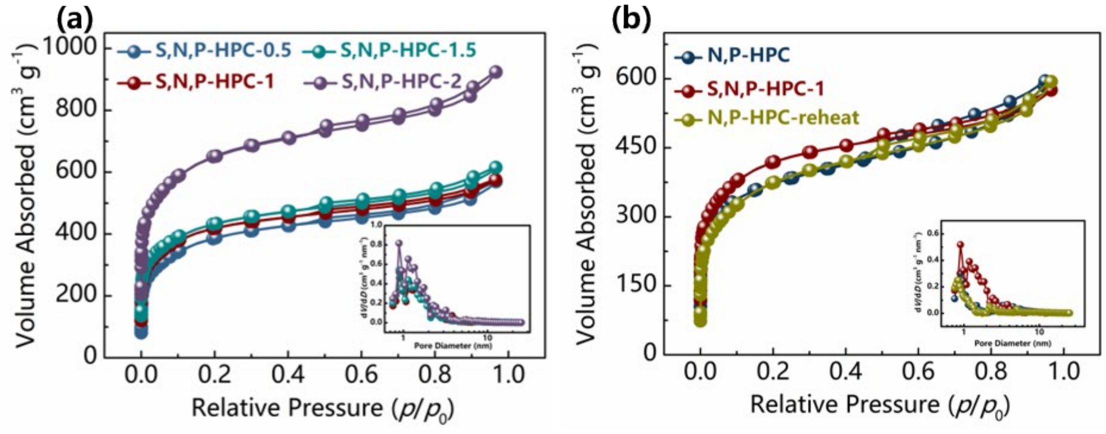

Figure S5. (a) Nitrogen adsorption-desorption isotherms of S,N,P-HPC-0.5, S,N,P-HPC-1, S,N,P-HPC-1.5, and S,N,P-HPC-2 (Inset in (a) is the corresponding DFT pore size distribution curves). (b) Nitrogen adsorption-desorption isotherms of N,P-HPC, S,N,P-HPC-1, and N,P-HPC-reheat (Inset in (b) is the corresponding DFT pore size distribution curves).

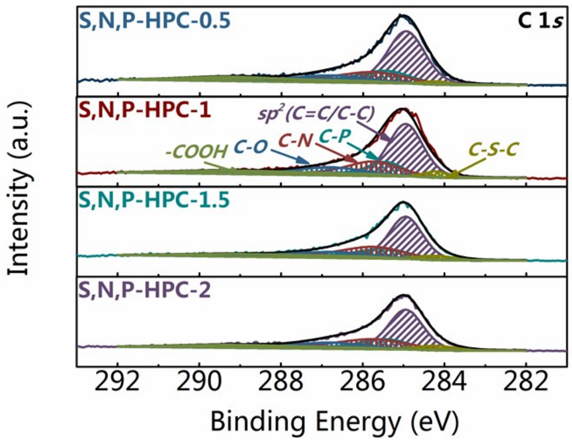

Figure S6. High-resolution XPS spectra of C *1s* for S,N,P-HPC-0.5, S,N,P-HPC-1, S,N,P-HPC-1.5, and S,N,P-HPC-2.

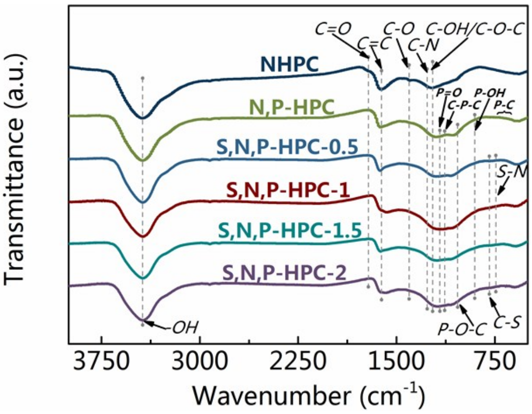

Figure S7. FT-IR spectra of NHPC, N,P-HPC, S,N,P-HPC-0.5, S,N,P-HPC-1, S,N,P-HPC-1.5, and S,N,P-HPC-2.

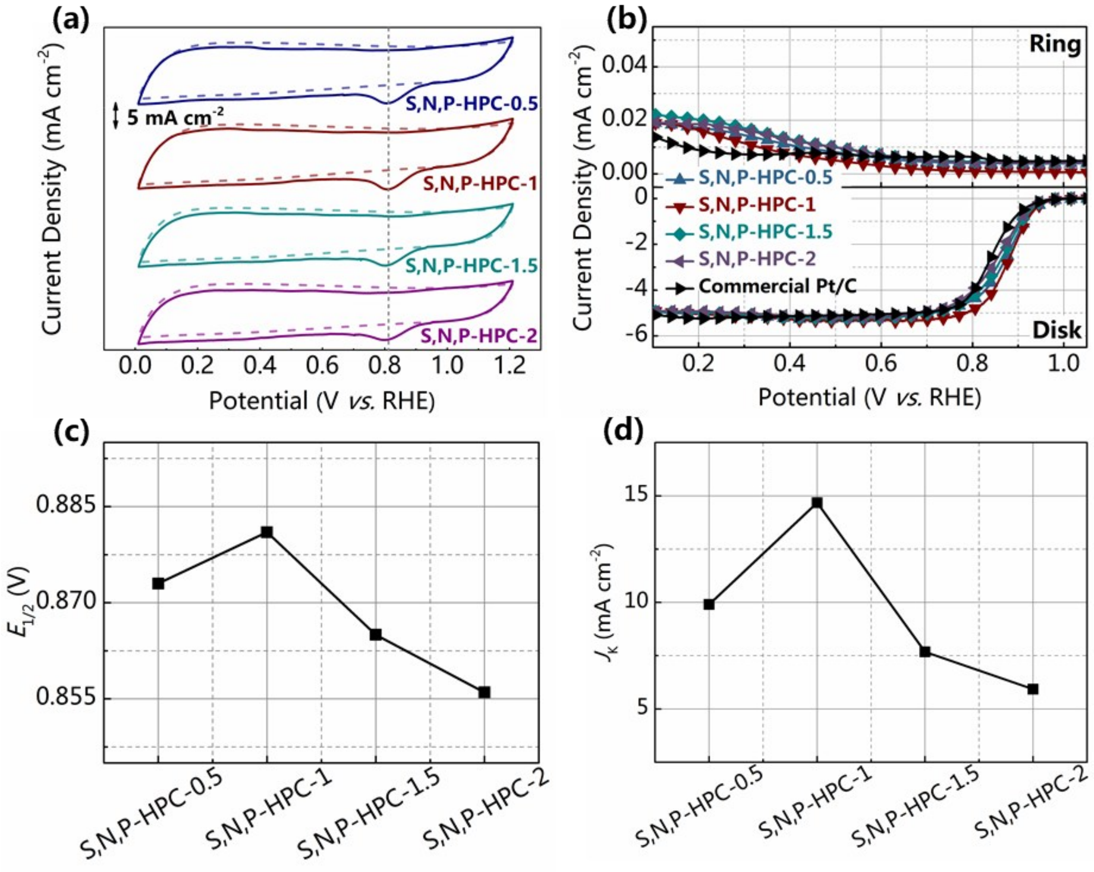

Figure S8. (a) CV curves of S,N,P-HPC prepared with different molar ratios of P/S of 1:2 (denoted as S,N,P-HPC-0.5), 1:1 (S,N,P-HPC-1), 3:2 (S,N,P-HPC-1.5), and 2:1 (S,N,P-HPC-2) in N_2- (dotted line) and O_2 -saturated (solid line) 0.1 M KOH (scan rate: 50 mV s^{-1}). (b) The corresponding RRDE voltammograms of the above samples and the commercial Pt/C in O_2-saturated 0.1 M KOH (scan rate: 5 mV s^{-1}; rotation rate: 1600 rpm). Summary of (c) $E_{1/2}$ and (d) J_k for S,N,P-HPC-0.5, S,N,P-HPC-1, S,N,P-HPC-1.5, and S,N,P-HPC-2.

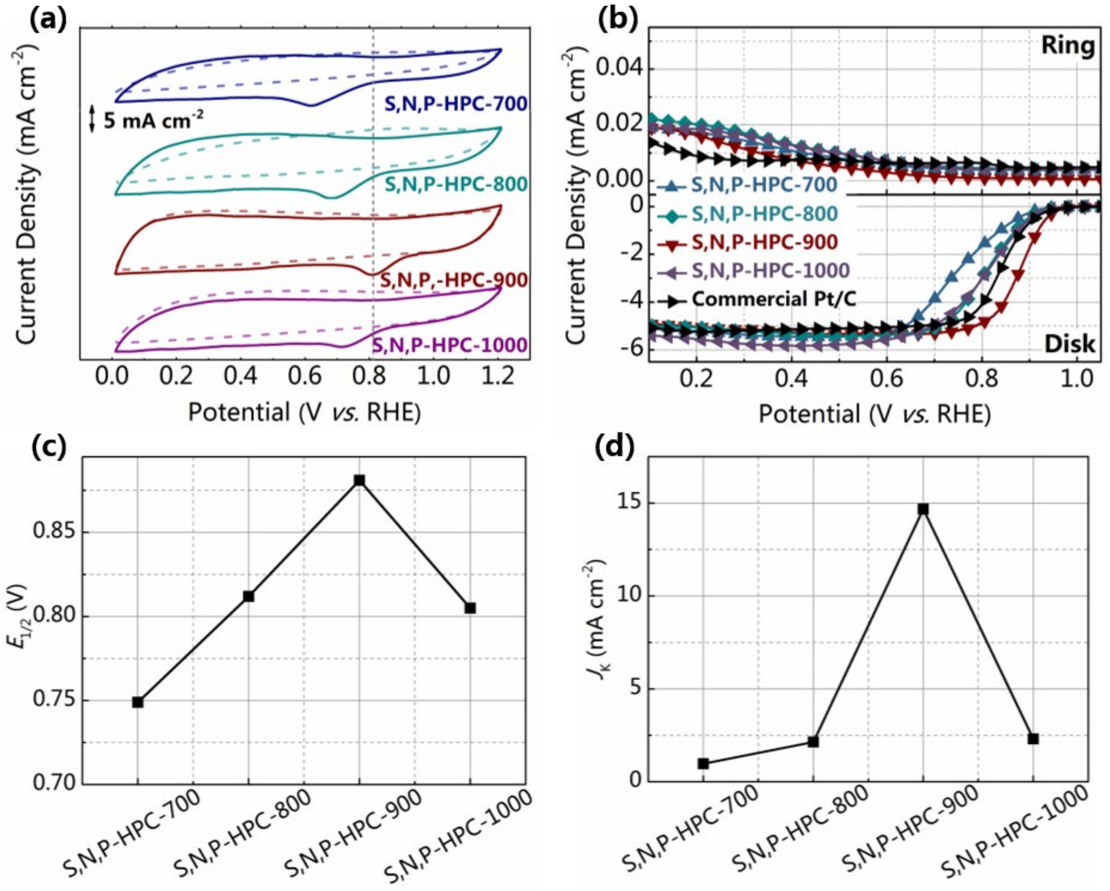

Figure S9. (a) CV curves of S,N,P-HPC-1 prepared at different pyrolysis temperature in N_2- (dotted line) and O_2-saturated (solid line) 0.1 M KOH (scan rate: 50 mV s^{-1}). (b) The corresponding RRDE voltammograms of the above samples and the commercial Pt/C in O_2-saturated 0.1 M KOH (scan rate: 5 mV s^{-1}; rotation rate: 1600 rpm). Summary of (c) $E_{1/2}$ and (d) J_k for S,N,P-HPC-700, S,N,P-HPC-800, S,N,P-HPC-900, and S,N,P-HPC-1000.

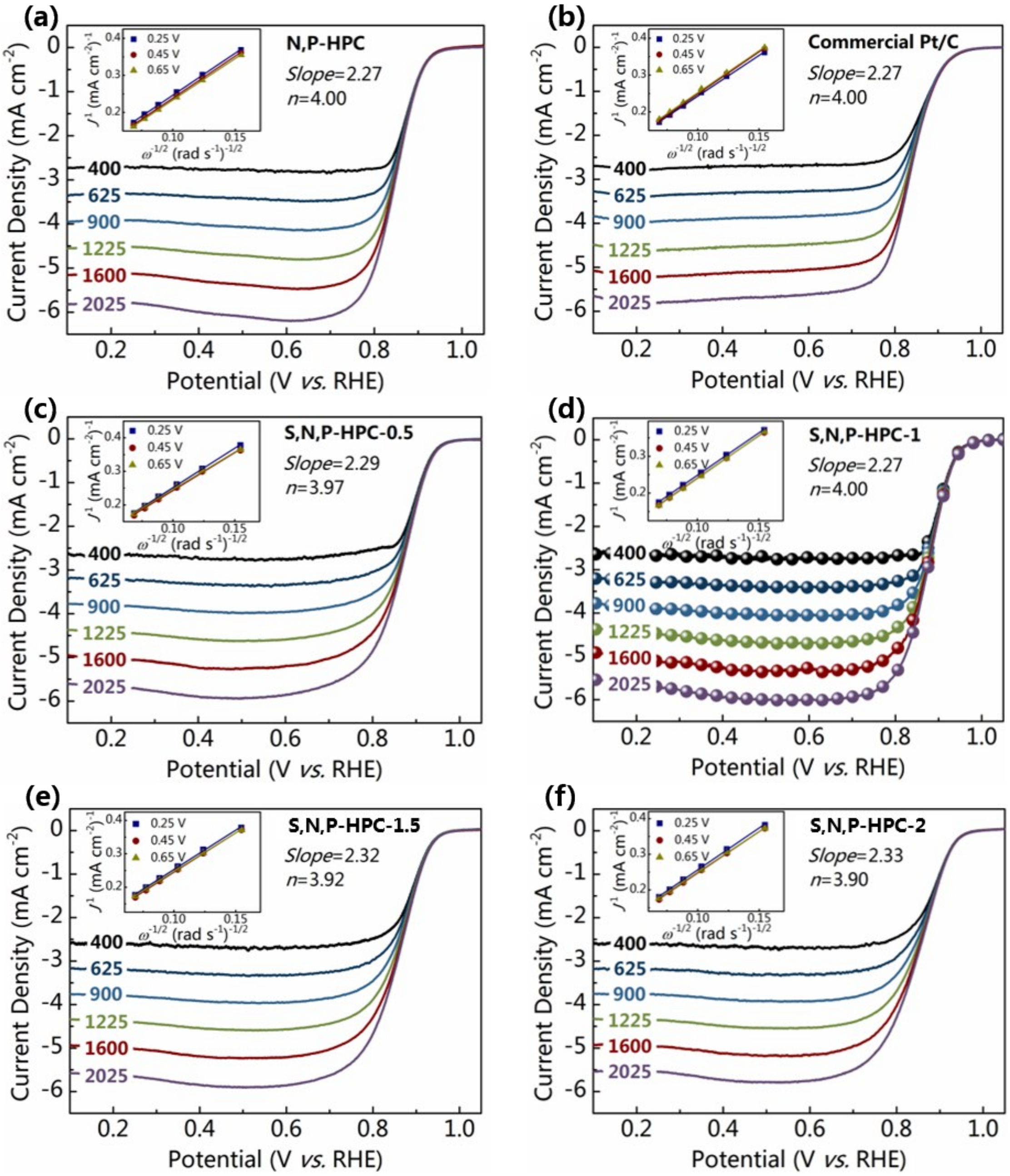

Figure S10. LSV curves of (a) N,P-HPC, (b) commercial Pt/C, (c) S,N,P-HPC-0.5, (d) S,N,P-HPC-1, (e) S,N,P-HPC-1.5 and (f) S,N,P-HPC-2 in O_2-saturated 0.1 M KOH (scan rate: 5 mV s^{-1}) at various rotation rates (400-2025 rpm) (Inset shows the corresponding K-L plots).

3. Supplementary Tables

Table S1. Pore structure characterization of NHPC, N,P-HPC, N,P-HPC-reheat and a series of S,N,P-HPC samples.

Samples	S_{BET} (m^2 g^{-1})	S_{micro} (m^2 g^{-1})	V_{total} (cm^3 g^{-1})	V_{micro} (cm^3 g^{-1})	% V_{meso}
NHPC	2165	1278	1.869	0.7345	60.7
N,P-HPC	1516	1076	0.9834	0.4415	55.1
N,P-HPC-reheat	1482	999	0.8349	0.4208	49.6
S,N,P-HPC-0.5	1517	1188	0.9586	0.5052	47.3
S,N,P-HPC-1	1533	1165	0.8903	0.4932	44.6
S,N,P-HPC-1.5	1582	1191	0.9515	0.5071	46.7
S,N,P-HPC-2	2378	1769	1.429	0.7502	47.5

Table S2. Element contents of NHPC, N,P-HPC and a series of S,N,P-HPC samples determined by XPS.

Samples	Atomic composition (at.%)				
	C	O	N	P	S
NHPC	80.09	17.41	2.50	0	0
N,P-HPC	76.00	16.84	3.20	3.96	0
S,N,P-HPC-0.5	81.37	10.79	3.69	2.59	1.56
S,N,P-HPC-1	80.35	11.31	4.35	2.96	1.29
S,N,P-HPC-1.5	81.32	9.36	4.46	3.3	1.56
S,N,P-HPC-2	80.36	11.19	3.62	3.52	1.3

Table S3. The relative contents of different N species from high-resolution N 1*s* spectra.

Samples	Relative content of different N species to total N (%)			
	Pyridinic N	**Pyrrolic N**	**Graphitic N**	**Oxidized pyridinic N**
NHPC	43.67	26.84	10.68	18.81
N,P-HPC	55.65	17.08	10.24	17.03
S,N,P-HPC-0.5	31.28	9.24	34.96	24.52
S,N,P-HPC-1	49.37	8.20	33.35	9.08
S,N,P-HPC-1.5	33.21	4.49	30.77	31.53
S,N,P-HPC-2	27.98	7.52	33.99	30.51

Table S4. The relative contents for different P species from high-resolution P 2*p* spectra.

Samples	Relative content of different P species to total P (%)	
	P-C	**P-O**
N,P-HPC	66.88	33.12
S,N,P-HPC-0.5	52.69	47.31
S,N,P-HPC-1	79.36	20.64
S,N,P-HPC-1.5	65.15	34.85
S,N,P-HPC-2	58.33	41.67

Table S5. The relative contents for different S species from high-resolution S 2*p* spectra.

Samples	Relative content of different S species to total S (%)				
	-C-S-C-	**-C=S-**	**-C-SO_2-C-**	**-C-SO_3-C-**	**-C-SO_4-C-**

S,N,P-HPC-0.5	26.70	38.63	13.53	16.68	4.46
S,N,P-HPC-1	24.07	58.71	4.83	7.27	5.12
S,N,P-HPC-1.5	41.01	25.39	13.47	17.27	2.86
S,N,P-HPC-2	45.80	25.67	13.23	11.56	3.74

Table S6. Summary of ORR performance in alkaline electrolyte (0.1 M KOH) for recently reported metal-free electrocatalysts in the literatures.

Electrocatalyst	**Loading (μg cm^{-2})**	**$E_{1/2}$ (V)**	**J_k (mA cm^{-2}) @ 0.85 V**	**n**	**Ref.**
P,S-CNS	150	~0.870	12.170	~4	[S1]
LY-1000	-	0.760	1.262	3.78	[S2]
CNPS-900	152	0.647^{a}	0.10 ^{a}	2.99^{a}	[S3]
NPS-CNS-300-1000	600	0.800	0.941	3.8-4.0	[S4]
PS-CNF	200	0.860	8.584	~4.02	[S5]
NPS-C-MOF-5	102	0.765^{b}	0.724^{b}	3.5-3.9^{b}	[S6]
NSP-PC-2	400	0.850	5.5	3.84	[S7]
NSC/MPA-5	250	0.760	0.809	3.58-3.99	[S8]
PSNG1:10	280	0.9031^{a}	16.467^{a}	3.81^{a}	[S9]
GNSP-31	-	0.805^{b}	2.911^{b}	~4^{b}	[S10]
CDs/M-rGO	102	0.802^{a}	0.999^{a}	3.7-4.0^{a}	[S11]
NPSC	204	0.753	0.890	3.83-3.92	[S12]
WWCNRs	-	0.99^{c}	5.876^{c}	3.6-3.8^{c}	[S13]
yolk-CN-800	354	0.765^{b}	0.010^{b}	~4.0^{b}	[S14]
BNPS-Gr	300	0.765^{b}	0.455^{b}	~3.7^{b}	[S15]

BNPGA-1000-15	600	0.775[b]	1.119[b]	3.7[b]	[S16]
NPBC-2	100	0.762[a]	0.563[a]	~3.6[a]	[S17]
BNP-GnPs	283	0.625[b]	0.001[b]	3.9[b]	[S18]
NBCNHm	1132	0.625[b]	0.001[b]	4.0[b]	[S19]
GO-PANi31-FP	-	0.72	0.430	3.85	[S20]
N–S–B-CNTs	224	0.765[b]	0.010[b]	3.98-4.02[b]	[S21]
N,S,O-OMC	150	0.750	3.42	3.5	[S22]
NHPC	800	0.740	0.081	3.30	This work
N,P-HPC	800	0.853	6.049	4.00	This work
S,N,P-HPC-0.5	800	0.873	9.908	3.97	This work
S,N,P-HPC-1	800	0.881	14.680	4.00	This work
S,N,P-HPC-1.5	800	0.865	7.679	3.92	This work
S,N,P-HPC-2	800	0.856	5.930	3.90	This work
Commercial Pt/C	400	0.841	3.826	4.00	This work

Note: All the SCE[a], Ag/AgCl[b] and Hg/HgO[c] potentials have been converted to the RHE potential.

References

[S1] S. S. Shinde, C. H. Lee, A. Sami, D. H. Kim, S. U. Lee and J. H. Lee, *ACS Nano.*, 2016, **11**, 347-357.

[S2] F. Razmjooei, K. P. Singh and J. S. Yu, *Catal. Today*, 2016, **260**, 148-157.

[S3] S. Dou, A. Shen, Z. Ma, J. Wu, L. Tao and S. Wang, *J. Electroanal. Chem.*, 2015,

753, 21-27.

[S4] Y. N. Zhu, C. Y. Cao, W. J. Jiang, S. L. Yang, J. S. Hu, W. G. Song and L. J. Wan, *J. Mater. Chem. A*, 2016, **4**, 18470-18477.

[S5] S. S. Shinde, J. Y. Yu, J. W. Song, Y. H. Nam, D. H. Kim and J. H. Lee, *Nanoscale Horiz.*, 2017, **2**, 333-341.

[S6] J.-S. Li, S.-L. Li, Y.-J. Tang, K. Li, L. Zhou, N. Kong, Y.-Q. Lan, J.-C. Bao and Z.-H. Dai, *Sci. Rep-UK*, 2014, **4**, 5130.

[S7] K. Chen, Y. Hao, M. Zhang, D. Zhou, Y. Cao, Y. Wang and L. Feng, *RSC Adv.*, 2017, **7**, 5782-5789.

[S8] A. Mulyadi, Z. Zhang, M. Dutzer, W. Liu and Y. Den, *Nano Energy*, 2017, **32**, 336-346.

[S9] Y. Wang, B. Zhang, M. Xu and X. He, *RSC Adv.*, 2015, **5**, 86746-86753.

[S10] F. Razmjooei, K. P. Singh, M. Y. Song and J. S. Yu, *Carbon*, 2014, **78**, 257-267.

[S11] L. Zhou, P. Fu, Y. Wang, L. Sun and Y. Yuan, *J. Mater. Chem. A*, 2016, **4**, 7222-7229.

[S12] J. T. Ren and Z. Y. Yuan, *Chemcatchem*, 2018, **10**, 3260-3268.

[S13] S. Gao, X. Wei, H. Liu, K. Geng, H. Wang, H. Moehwald and D. Shchukin, *J. Mater. Chem. A*, 2015, **3**, 23376-23384.

[S14] Z. Shao, W. Zhang, D. An, G. Zhang and Y. Wang, *Rsc Adv.*, 2015, **5**, 97508-97511.

[S15] M. A. Molina-García and N. V. Rees, *Appl. Catal. A- Gen.*, 2018, **553**, 107-116.

[S16] H. Lin, L. Chu, X. Wang, Z. Yao, F. Liu, Y. Ai, X. Zhuang and S. Han, *New J. Chem.*, 2016, **40**, 6022-6029.

[S17] S. Zhao, J. Liu, C. Li, W. Ji, M. Yang, H. Huang, Y. Liu and Z. Kang, *ACS Appl. Mater. Inter.*, 2014, **6**, 22297-22304.

[S18] P. Routh, S. H. Shin, S. M. Jung, H. J. Choi, I. Y. Jeon and J. B. Baek, *Eur. Polym. J.*, 2018, **99**, 511-517.

[S19] X. Wu, L. Liu, P. Tang, M. Li and Z. Shi, *RSC Adv.*, 2016, **6**, 63730-63735.

[S20] J. Zhang and L. Dai, *Angew. Chem.-Int. Edit.*, 2016, **55**, 13296-13300.

[S21] S. Liu, G. Li, Y. Gao, Z. Xiao, J. Zhang, Q. Wang, X. Zhang and L. Wang, *Catal. Sci. Technol.*, 2017, **7**, 4007-4016.

[S22] J. Y. Cheon, J. H. Kim, J. H. Kim, K. C. Goddeti, J. Y. Park, and S. H. Joo, *J. Am. Chem. Soc.*, 2014, **136**, 8875-8878.